

AD-A039 240

GENERAL ELECTRIC CORPORATE RESEARCH AND DEVELOPMENT --ETC F/G 9/4
ESTIMATION OF THE DETECTION PERFORMANCE OF A DISPLAY.(U)

JAN 75 D E WOOD

N00014-71-C-0229

UNCLASSIFIED

SRD-75-063

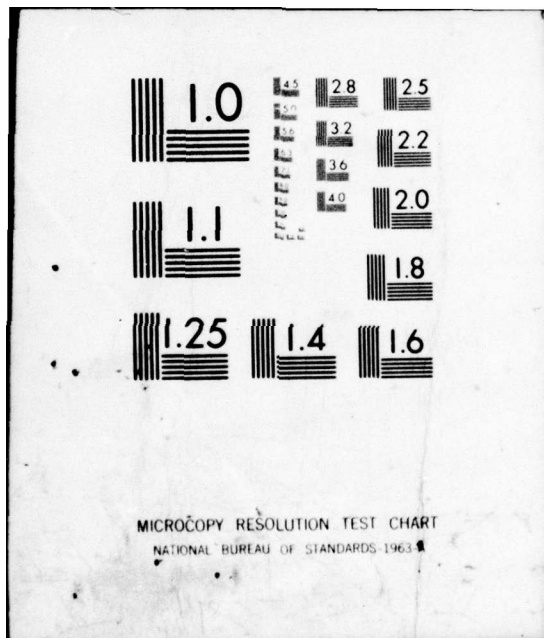
NL

| OF |
AD
A039240



END

DATE
FILMED
6-77



ADA 039240

6 ESTIMATION OF THE DETECTION PERFORMANCE
OF A DISPLAY

7 TECHNICAL REPORT TO OFFICE OF NAVAL RESEARCH

Contract No. N00014-71-C-0229

15

10 D.E. Wood

11 15 Jan 1975

12 21p.

DISTRIBUTION STATEMENT A

Approved for public release;
Distribution Unlimited

General Electric Company
Corporate Research and Development
Schenectady, N.Y. 12301

14 SRD-75-063



406 617

NO FILE COPY

ESTIMATION OF THE DETECTION PERFORMANCE OF A DISPLAY

Signal detection performance is commonly described by "Receiver Operating Characteristic" (ROC) curves plotting the probability of signal detection (PD) versus the probability of false alarm (PFA) over a range of detection thresholds.* This report describes a method for determining ROC curves for visual displays and presents results obtained from display evaluations.

The visible displays discussed here will represent functions derived from a meaningless random noise waveform that has a particular controlled waveform added whenever a "signal plus noise" message is to be displayed. The addition of signal will be detected by the change in visible patterns from a meaningless noise background to a significantly ordered pattern.

The signal-to-noise ratios are the relative power in the signal and noise waveforms combined to create signal messages.

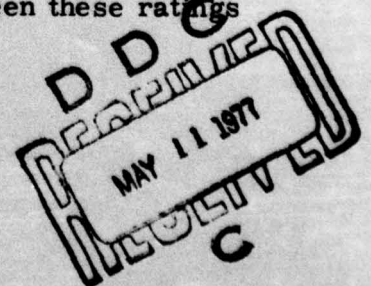
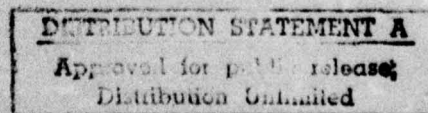
Method for Obtaining ROC Curves for Visual Displays

The method is based on the following assumptions:

1. The observer can set a "threshold" which he can use to decide whether a "signal" is present. This threshold will determine the PD and PFA.
2. The observer can maintain a threshold through a sequence of observations.
3. The observer can change his threshold or equivalently can describe his degree of confidence that a signal is present.

Under these assumptions, a "rating scale" method will provide several points on an ROC curve from a single series of observations. The ratings are the observers' relative degree of confidence that a signal created the pattern observed. For example, an integer scale 0 through 10 may be used. The observer would rate an observation as 0 if he saw no evidence at all of signal. A rating of 5 would indicate the observers' feeling that no signal or signals were equally probable. A 10 rating would signify unqualified confidence that a signal exists. Degrees of confidence between these ratings would be recorded as intervening integers.

*See Bibliography.



The rationale for using a rating scale to obtain points on an ROC curve can be explained in terms of probability density distributions. Assume that a detection function has one probability density distribution for noise and a different distribution for signal plus noise as shown in Figure 1. Now assume that a detection function threshold is established as shown. The area under the portion of the S + N probability density distribution curve to the right of the threshold is the PD. Correspondingly, the PFA is the area under the portion of the noise only curve to the right of the threshold. By selecting a series of threshold points one can determine the PD and PFA curves as a function of threshold settings.

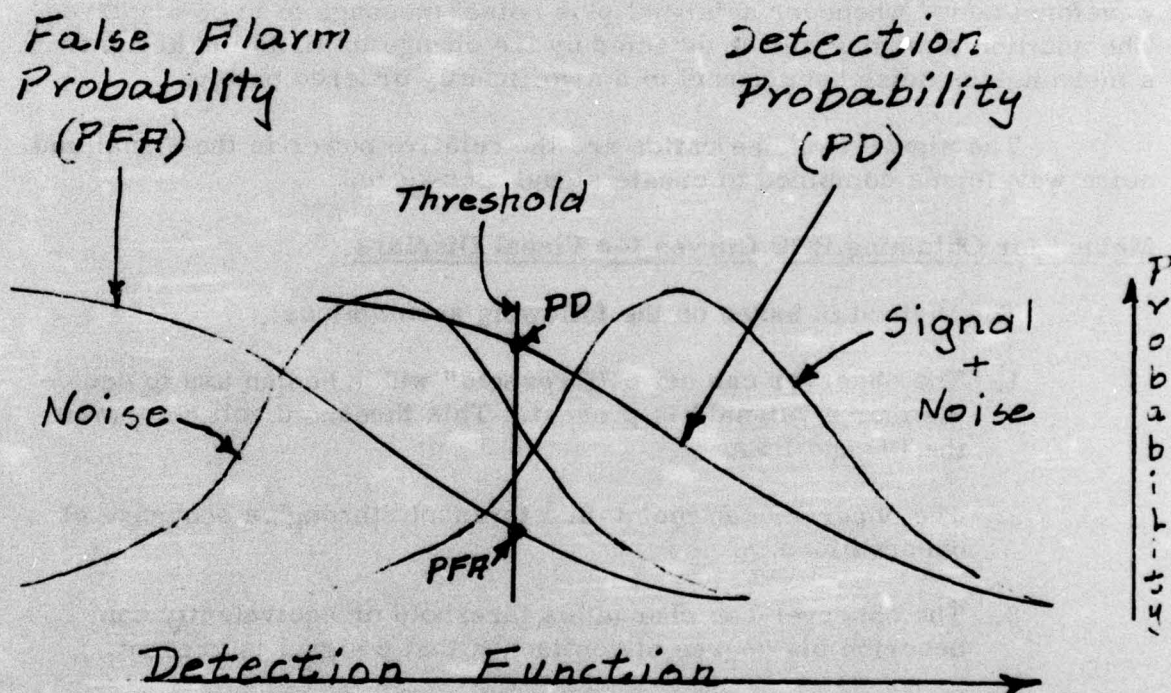


Figure 1 Signal detection relations.

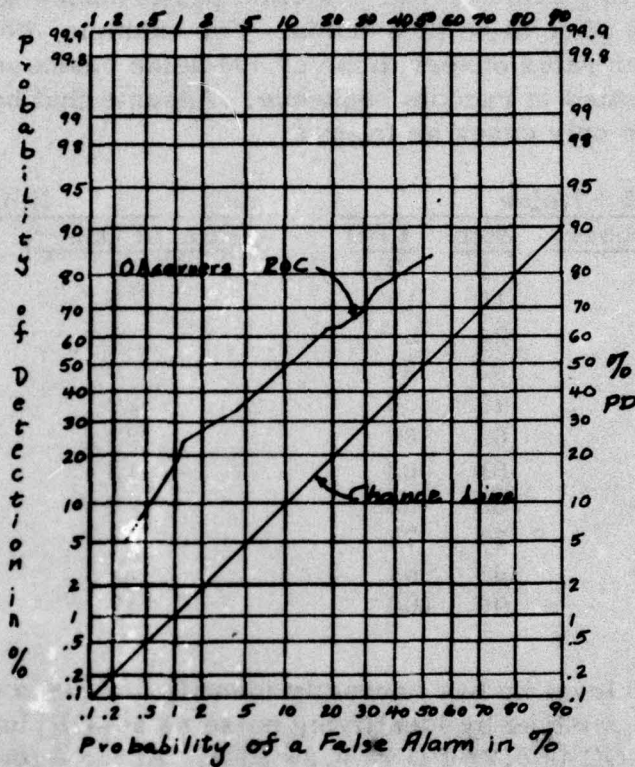


Figure 2 Visual display ROC curve.

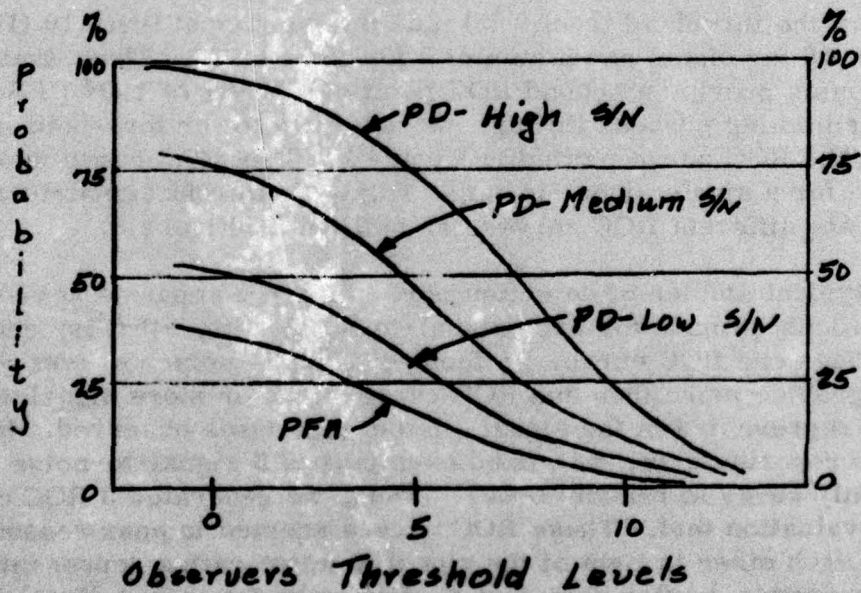


Figure 3 Rating scale relations.

Detection Performance for Intensity Modulated Spectrograms

Time history displays of signal spectra representing amplitude gray scale shadings (Kay Sonagraph, etc.) are widely used in signal processing studies. The spectrograms evaluated here were made by passing signals through an analog spectrum analyzer and recording the spectra on 35 mm strip film by photographing a C. R. T. display. The amplitude function recorded is the magnitude of the spectrum as a function of frequency. Continuous film motion produces a time history record of successive spectra.

For display evaluation, a random noise generator supplied the "noise only" conditions. A sine wave of constant frequency and known power was added to the random noise for signal plus noise cases. Three signal-to-noise ratios were selected to span the general region of 10% to 90% PD for a PFA of about 2%. A total of 600 cases were prepared--approximately 300 noise only and about 100 each at the three signal-to-noise ratios. Observer endurance and the cost of testing limited both the number of sample observations and the number of observers.

Each test sample was a piece of 35 mm film. Figures 4a, 4b, 4c and 4d reproduce samples that were shown to the observer for training prior to testing. Each film section represents a time bandwidth product of about 70 over a frequency span of about 40 spectral lines (resolution elements). If present, the sine wave signal would appear at the center of the frequency range (vertical). Thus, the general background was always random noise. The actual test samples were mounted individually on cards placed in a rotary file. The rotary file presents only one card in view at a time, preventing comparisons of different test samples. Each card was numbered for use by the observer in rating and for use by the scorer in calculating ROC curves. The 600 samples were divided into 5 groups of 120 samples each. The observer does only one group at a time to avoid fatigue. Our experience shows that an experienced observer can estimate probabilities for 120 test cases in about 15 minutes.

The following rating scale instructions were given to each observer on a sheet which he kept with him during the tests.

<u>Rating</u>	<u>Meaning</u>
10	Absolutely sure target is present
9	
8	
7	
6	
5	50% probability target is present
4	
3	
2	
1	Hint of target
0	See no indication target is present

WT ~ 70

NOISE

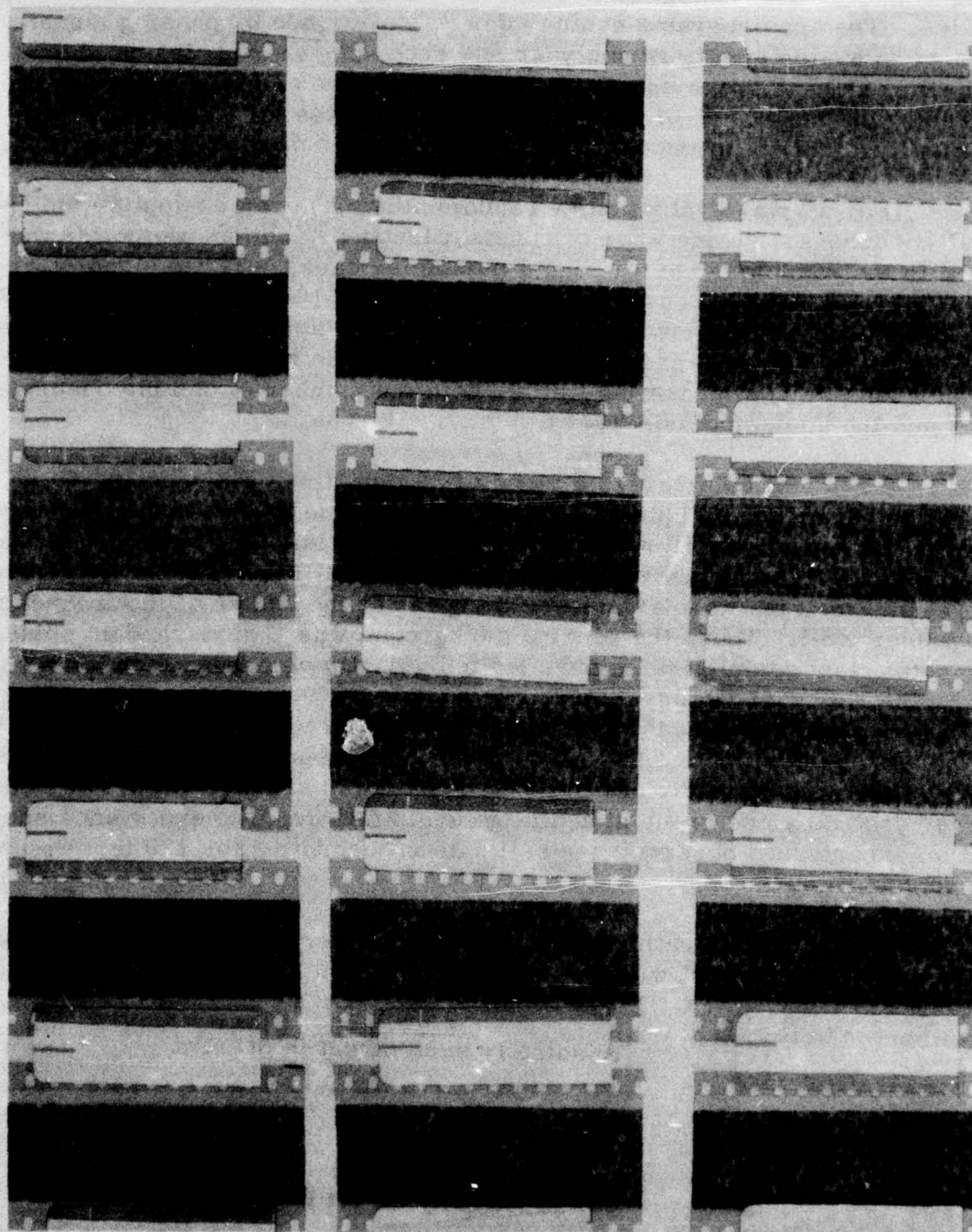


Figure 4-A.

WT ~70 LOW S/N (-5 db IN FILTER BAND)

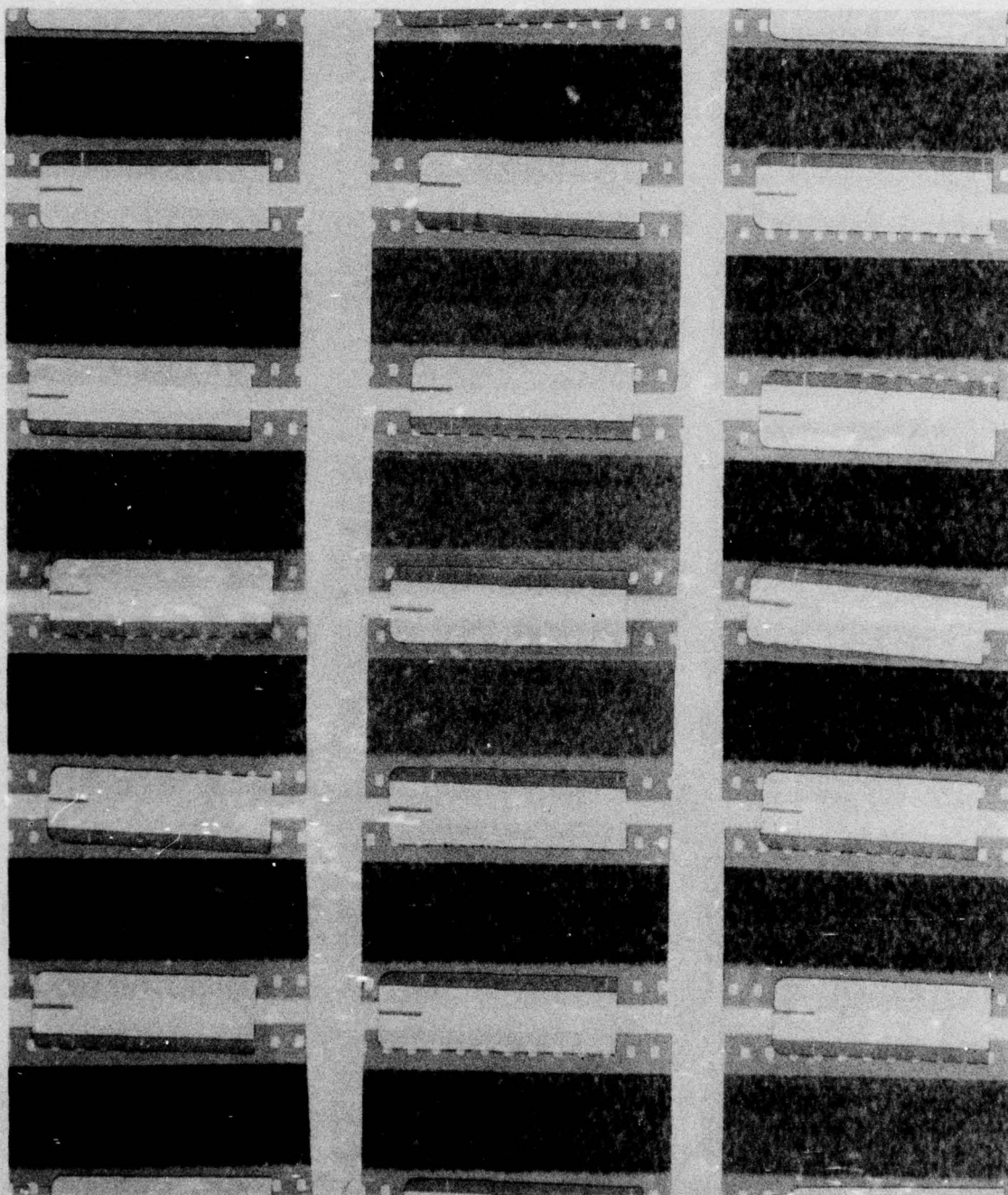


Figure 4-B.

WT ~70

MEDIUM S/N (-2.0 db IN FILTER BAND)

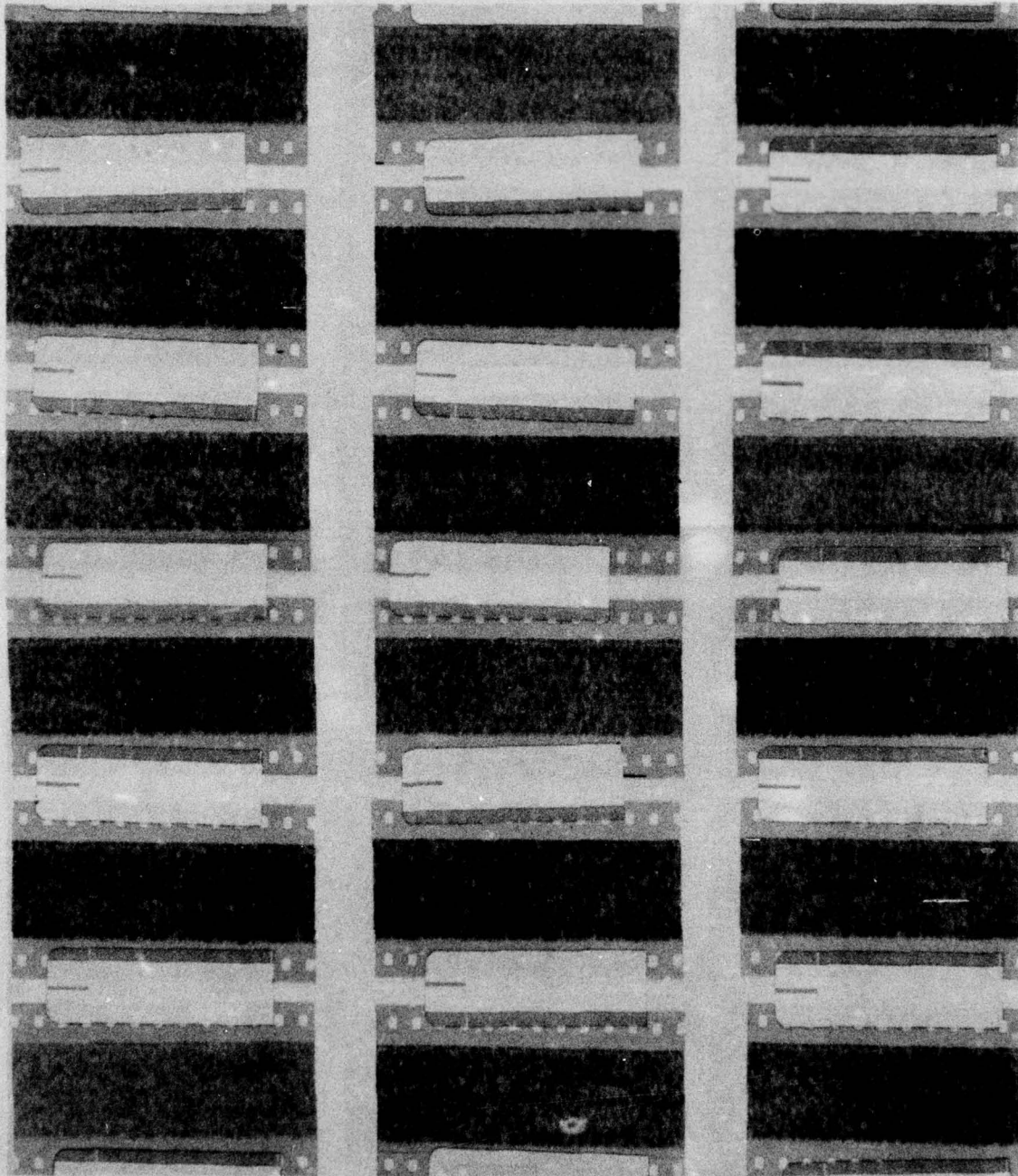


Figure 4-C

WT ~70

HIGH S/N (+ 1.0 db IN FILTER BAND)

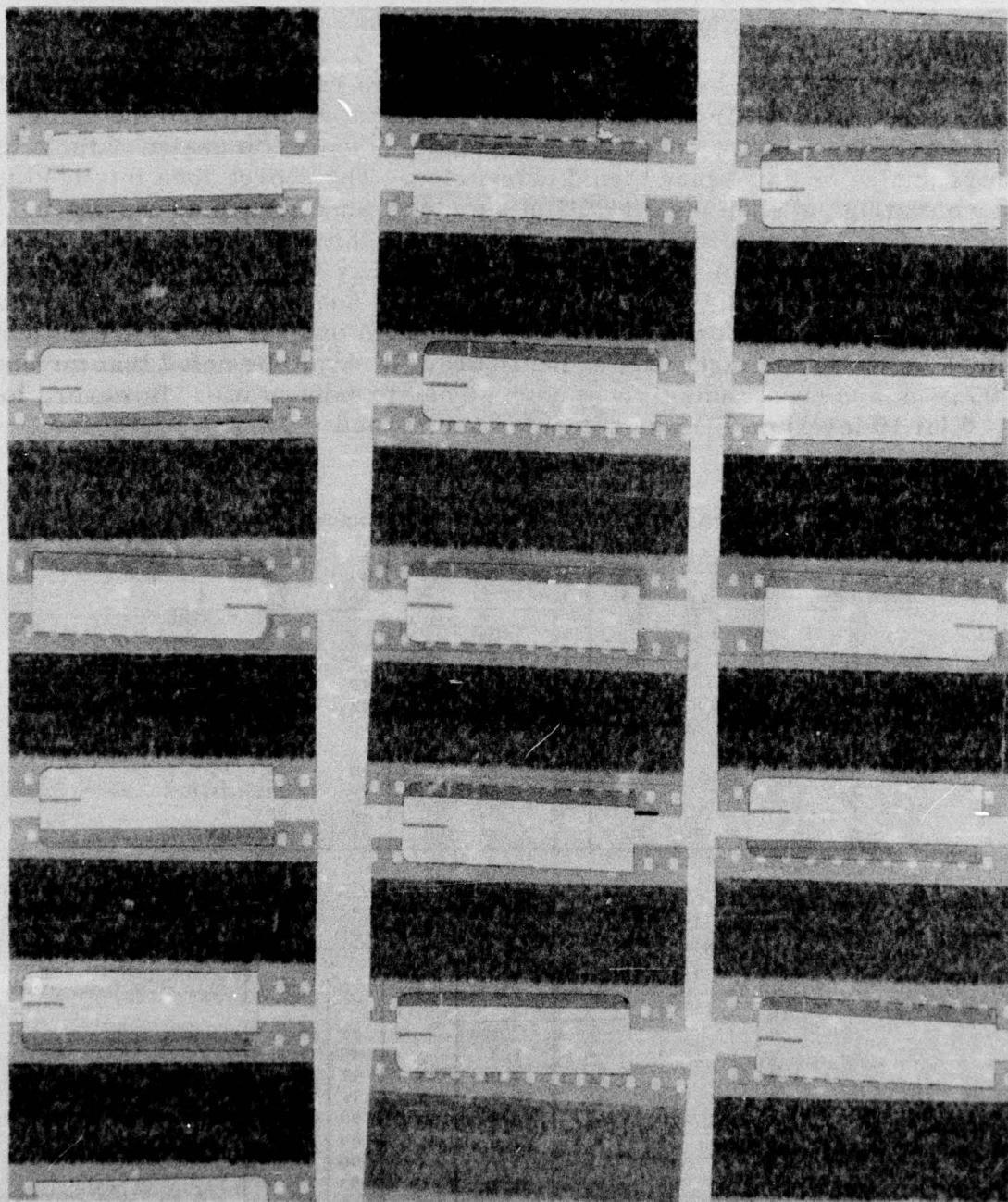


Figure 4-D.

The observer was instructed orally to use all the rating levels as suitable. Test case samples (Figure 4) were shown to the observer before a test. The observer could examine these samples for as long as he chose, but the training sheet was removed before the test began. All of the observers for this particular display evaluation were already acquainted with the interpretation of the intensity modulated spectrogram.

Computing ROC curves from the observers ratings was done manually. The observers wrote their probability ratings in spaces numbered the same as the test cards. Master code sheets enabled the scorer to assign ratings to the proper noise or noise plus signal categories. The scorer then totalized the number of ratings at each level to fill in summary sheets such as the one in Figure 5. For each condition--noise only and the three signal-to-noise ratios--the number of cases rated at each level of probability (0 through 10), the cumulative sums going from the highest level to lowest, and the % of the total number of cases in a category is calculated. The final PFA and PD values are collected in a block on the lower right part of the figure. It should be noted that for each PFA there is a corresponding PD at each signal-to-noise ratio. However, for PFA = 0 (at 10 level) no PD was computed and plotted.

SUMMARY SHEET FOR PLOT OF OBSERVERS ROC

Probability	S/N = 1			S/N = 2			S/N = 3		
	Num- ber	Σ	%	Num- ber	Σ	%	Num- ber	Σ	%
10	52	52	58	4	4	4.17	1	1	.945
9	19	71	79.4	18	22	23	6	7	6.6
8	10	81	90.3	12	34	35.4	5	12	11.3
7	2	83	92.5	11	45	47	16	28	26.6
6	4	87	97	23	68	70.6	12	40	37.7
5	2	89	99	12	80	83.2	9	49	46.3
4	0			5	85	88.7	11	60	56.6
3	0			1	86	90	10	70	66
2	0			3	89	93	9	79	74.6
1	0			4	93	97	13	92	87
0	1	90	100	3	96	100	14	106	100

Probability	N Num- ber	Σ	PFA	PD		
			N	1	2	3
10	0	0	0			
9	1	1	.325	79.4	23	6.6
8	3	4	1.3	90	35	11.3
7	7	11	3.58	92.5	47	27
6	20	31	10.2	97	71	38
5	20	51	16.7	99	83	46
4	19	70	22.8		89	57
3	13	83	27		90	66
2	35	118	38.6		93	75
1	66	184	60		97	87
0	124	308				

Figure 5.

The calculated ROC curves for four observers are reproduced in Figure 6. There are three sets of ROC plots representing three different signal-to-noise conditions. There is good agreement among observers' estimates of the ROC curve as shown by the clustering of plots for a particular signal-to-noise and the clear separation between clusters of plots for the signal-to-noise ratios which differed in 3 db steps. One observer (HS) applied a restricted range of thresholds relative to the other three observers, but his "short" ROC curves coincide with corresponding parts of the other plots.

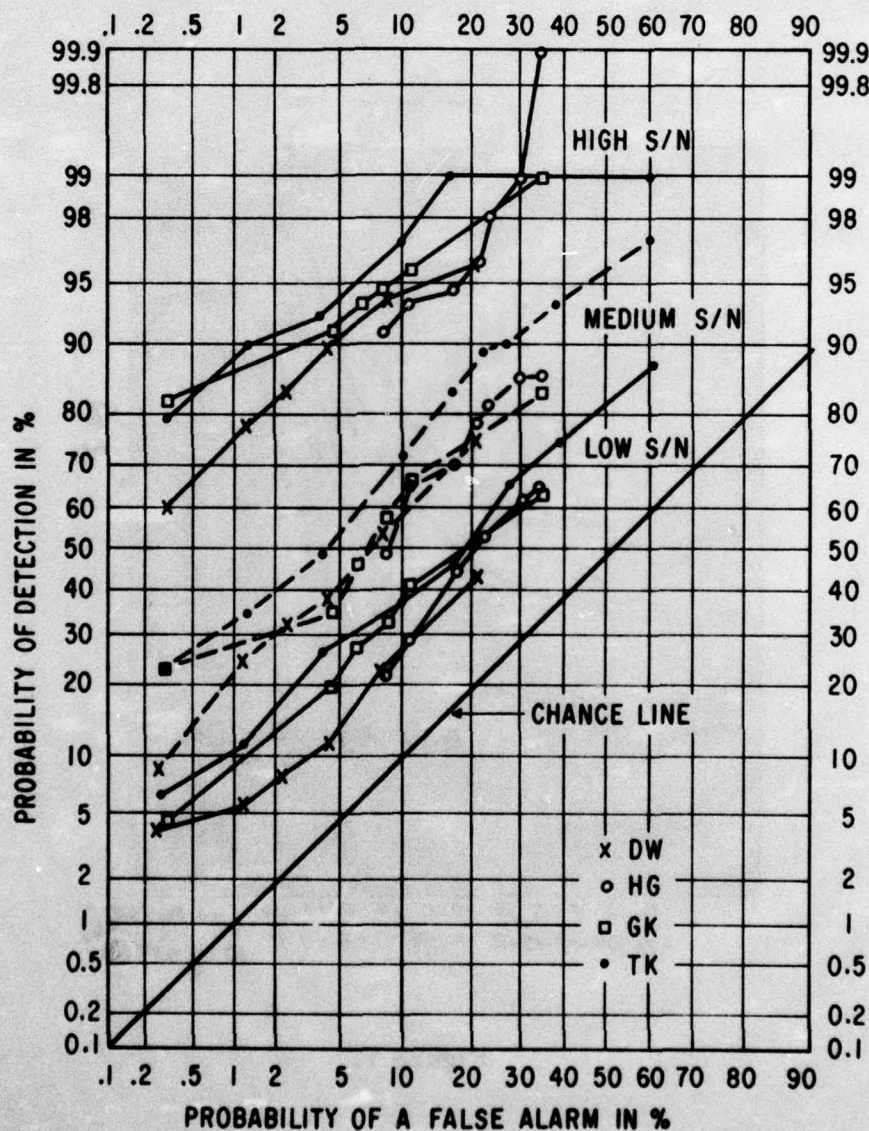


Figure 6.

A comparison of these ROC curves with theoretical detection performance* is shown in Figure 7. Theoretical curves are shown for $PFA = 0.01, 0.1, \text{ and } 0.3$. Corresponding "mean" values are shown for the spectrogram ROC curves. The time-bandwidth products ($wt = 60$ vs 70) are slightly different, but the error is negligible. The detection performance for the visual display seems to lie about 3 db below theoretical--a seemingly reasonable difference in the light of known imperfections in the spectrum analysis process used.

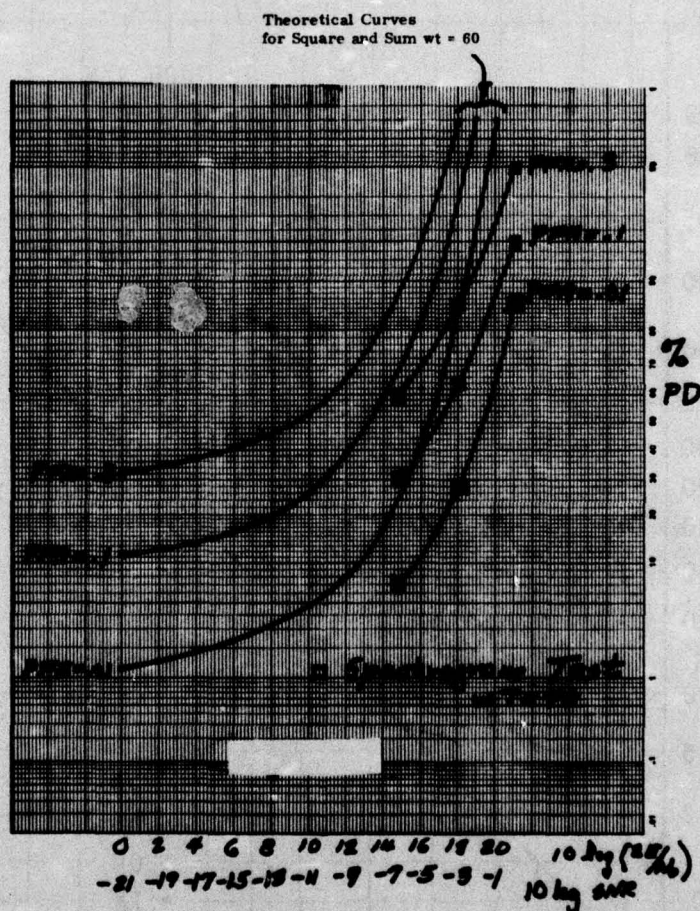


Figure 7.

*See Appendix A of this report for calculation of Square Law Detector Performance

Conclusions

The rating scale method for generating ROC curves of detection performance seems to have worked well here. Mixing cases with different signal-to-noise ratios generated ROC plots with detection performance that varied with expected relations, as shown by comparison to theoretical ROC. Since all of the observers examined the same test cases, the spread between ROC's is caused by differences between observers. Oddly enough, the most experienced observer (DW) had the lowest PD values. Certainly tests with more than four observers would be required to predict performance variation among observers.

BIBLIOGRAPHY

Books:

Psychoacoustics and Detection Theory - D.M. Green

**Contemporary Readings in Signal Detection and Recognition by
Human Observers - John A. Swets**

John Wiley & Sons

Articles and Reports:

Transactions of the Institute of Radio Engineers

Professional Group on Information Theory

PGIT-4 (1954) Symposium Record

"The Theory of Signal Detectability", Petersen, Birdsall, Fox

"The Human Use of Information", Tanner, Swets

JASA, 1958, Vol. 30, pp 922-928

**"Definition of d' and n as Psychophysical Measures", Tanner,
Birdsall**

JASA, 1960, Vol. 32, pp 1189-1203

"Psychacoustics and Detection Theory" - David M. Green

JASA, 1959, Vol. 31, pp 1031

"On Indices of Signal and Response Discriminability", Irwin Pollack

JASA, 1964, Vol. 36, pp 766-774

"Stimulus Oriented Approach to Detection", Lloyd A. Jeffries

JASA, 1961, Vol. 33, pp. 993-1007

**"Operating Characteristics, Signal Detection, and the Method of
Free Response", Egan, Greenberg, Schulman**

Electronic Defense Group Tech. Report #3, Ann Arbor

Electronic Defense Group, The Univ. of Michigan, 1953

"The Theory of Signal Detectability", Peterson, Birdsall

Psychology Review 68, pp 301-340, 1961

"Decision Processes in Perception", Swets, Tanner, Birdsall

Psychology Review 63, pp 81-97, 1956

"Magical Number of 7, etc." E.A. Miller

JASA, Vol. 34, pp 172-178, 1962

"Ear vs Eye ROC"

JASA, Vol. 31, pp 629-630, 1959

"Types ROC", Clark, Birdsall, Tanner

Amer. Journal Psychology, Vol. 72, pp 503-520, 1959

"Statistically Refined Pattern in Matrix of Dots", Green, Wolf, White

JASA, Vol. 31, pp 243-244, 1959

"Graphical Presentation of Data in Framework of Theory of Signal Detection" Tanner

APPENDIX A

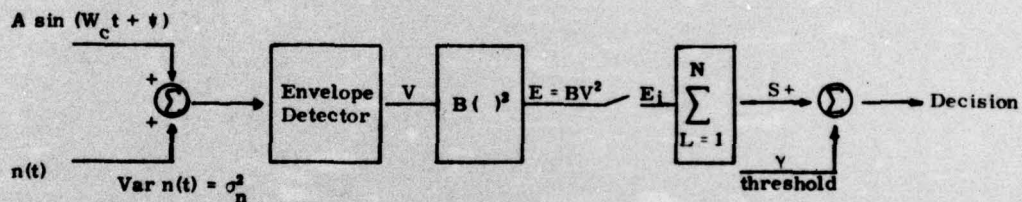
SQUARE LAW DETECTOR PERFORMANCE - by R. R. Rustay

This Appendix briefly describes the computational procedure used to obtain the curves on Figure 7. The computational procedure is based directly on the report

A Statistical Theory of Target Detection by Pulsed Radar:
Mathematical Appendix

J.I. Marcum, The Rand Corporation Report RM-753, 1 July 1948
Reissued 25 April 1952

The "square law" model being considered is shown in the following sketch*



where $n(t)$ is narrow band Gaussian noise centered about W_c and ψ is a random uniformly distributed $(0, 2\pi)$ constant. The probability density function (pdf) $Q_s(S/A)$ associated with sum S

$$Q_s(S/A) = \left(\frac{2\sigma_n^2}{A^2} = \frac{1}{N} \frac{S}{2B\sigma_n^2} \right)^{\frac{N-1}{2}} \frac{e^{-\frac{NA^2}{2\sigma_n^2}} e^{-\frac{S}{2B\sigma_n^2}}}{2B\sigma_n^2} I_{N-1} \left(2 \sqrt{\frac{NA^2}{2\sigma_n^2}} \sqrt{\frac{S}{2B\sigma_n^2}} \right), \quad S \geq 0$$

where

$L_{N-1}(\chi)$ = Modified Bessel Function of the First Kind

The noise alone (zero signal) pdf is

$$Q_s(S/0) = \frac{1}{(N-1)! \cdot 2B\sigma_n^2} \left(\frac{S}{2B\sigma_n^2} \right)^{N-1} \exp \left(-\frac{S}{2B\sigma_n^2} \right), \quad S \geq 0$$

*The constant B was included for purpose of normalizing if desired.

The mean \bar{S} and variance vars are

$$\bar{E} = N \left(2B\sigma_n^2 \right) \left[1 + \frac{A^2}{2\sigma_n^2} \right]$$

$$\sigma^2 = \text{Var } E = N \left(2B\sigma_n^2 \right) \left[1 + \frac{2A^2}{2\sigma_n^2} \right]$$

The probability of false alarm PFM is, given the threshold γ

$$\text{PFM} = \int_{\gamma}^{\infty} Q_s (S/0) ds = 1 - \frac{1}{(N-1)!} \int_0^{Y_B} y^{N-1} e^{-y} dy$$

and corresponding probability of detection PD

$$\text{PD} = \int_{\gamma}^{\infty} Q_s (S/A) ds = 1 - 2 \frac{e^{-q^2}}{q^{N-1}} \int_0^{\sqrt{Y_B}} y^N e^{-y^2} I_{N-1} (2\mu y) dy$$

where

$$q = \frac{NA^2}{2\sigma_n^2}$$

$$Y_B = \frac{\gamma}{2B\sigma_n^2}$$

PFM and PD can be expressed in terms of defined functions, i.e.,

$$\text{PFM} = 1 - I \left(\frac{Y_B}{N-1}, N-1 \right) = Q_{\chi^2} \left(2 Y_B / 2N \right)$$

$$\text{PD} = 1 - T_{\sqrt{Y_B}} \left(2N-1, N-1, \sqrt{q} \right)$$

where

$I(\mu, p)$ = Pearson's Incomplete Gamma Function

$Q_{\chi^2}(\chi^2 | \nu)$ = Complementary Chi-Square Probability Function

$T_y(m, n, r)$ = Incomplete Toronto Function

However, because tables of these functions are either not readily available or convenient, the integral

$$\int_r^\infty Q_S(S|A) ds$$

has been computed digitally using an Edgeworth form of a Gram-Charlier Series, i.e.,

$$\int_r^\infty Q_S(S|A) ds = \frac{1}{2} \text{ERFC}\left(\frac{T}{\sqrt{2}}\right) - \sigma C_3 \phi^{(3)}(T) - \sigma C_4 \phi^{(4)}(T) - \sigma C_6 \phi^{(6)}(T)$$

where

$$\sigma C_3 = \frac{1+3\chi}{3N^{1/2}(1+2\chi)^{3/2}} \quad \phi^{(2)}(T) = \frac{e^{-\frac{T^2}{2}}}{\sqrt{2\pi}} (T^2 - 1)$$

$$\sigma C_4 = \frac{1+4\chi}{4N(1+2\chi)^2} \quad \phi^{(3)}(T) = -\frac{e^{-\frac{T^2}{2}}}{\sqrt{2\pi}} (T^3 - 3T)$$

$$\sigma C_6 = \frac{(1+3\chi)^2}{18N(1+2\chi)^3} \quad \phi^{(5)}(T) = -\frac{e^{-\frac{T^2}{2}}}{\sqrt{2\pi}} (T^5 - 10T^3 + 15T)$$

$$\chi = \frac{A^2}{2\sigma_n^2} \quad T = \frac{y - \bar{E}}{\sigma} = \frac{Y_B - N(1+\chi)}{N^{1/2}(1+2\chi)}$$

$$\text{ERFC}(y) = 1 - \frac{2}{\sqrt{\pi}} \int_0^y e^{-t^2} dt$$

Computationally a PFM is selected, Y_B found by iteration, and then PD is computed for various signal-to-noise power ratios χ . Notice that the first term in the Gram-Charlier Series is the normal approximation.

R.RUSIAY1

PFMPD

05/16/74

11:48

```

00010      ERX=.00001
00020      IMAX=11
00030      SNMIN=0.
00040      SNMAX=20
00050      DDB=(SNMAX-SNMIN)/FLOAT(IMAX-1)
00060 100    PRINT:" "
00070      PRINT:"TYPE NUMBER N"
00080      READ:N
00090      IF(N.LE.0)STOP
00100 200    PRINT:" "
00110      PRINT:"TYPE PFM"
00120      READ:PFM
00130      IF(PFM.LE.0)GOTO100
00140      CONK=4.3429446*ALOG(FLOAT(2*N))
00150      XM2=FLOAT(N)
00160      XM1=XM2-1.0
00170      YM2=PFM-PROB(XM2,U.,N)
00180      YM1=PFM-PROB(XM1,U.,N)
00190      NCOUNT=0
00200 300    CONTINUE
00210      NCOUNT=NCOUNT+1
00220      X=YM1*(XM2-XM1)/(YM2-YM1)
00230      IF(ABS(X).LE.ERX)GOTO400
00240      IF(NCOUNT.GT.100)STOP
00250      XM2=XM1
00260      YM2=YM1
00270      XM1=XM1-X
00280      YM1=PFM-PROB(XM1,U.,N)
00290      GOTO300
00300 400    T=XM1-X
00310      PRINT:"]="=",I
00320      PRINT 440
00330 440-   FORMAT(2X,"N",5X,"PFM",5X,"PD",10X,"T",10X,"X",9X,"DB",
00340 8         5X,"DCK",4X,"100*PD")
00350      DO 500 I=1,IMAX
00360      DCK=SNMIN+FLOAT(I-1)*DDB
00370      DB=DCK-CONK
00380      X=10.**(.1*DB)
00390      PD=PROB(1,X,N)
00400      PRINT 450,N,PFM,PD,I,X,DB,DCK,100.*PD
00410 450-   FORMAT(13,1P5F11.3,0P2F8.2)
00420 500    CONTINUE
00430      GOTO200
00440      END
00450      FUNCTION PROB(T,X,N)
00460      XN=FLOAT(N)

```

```

00470      RN=SQRT(XN)
00480      OP2X=1.+2.*X
00490      SQOP=SQRT(OP2X)
00500      CI=(1-XN*(1.+X))/(RN*SQOP)
00510      TI=CI*CI
00520      CALL ERFC(.70/107*CI,EX,CX)
00530      CEXP=.3989423*EXP(-.5*TI)
00540      SC3=-(1.+5.*X)/(3.*RN*OP2X**1.5)
00550      SC4=(1.+4.*X)/(4.*XN*OP2X**2)
00560      SC6=(1.+3.*X)**2/(10.*XN*OP2X**3)
00570      H2=1T-1.0
00580      H3=CI*(1T-3.0)
00590      H5=CI*((1T-10.0)*1T+15.0)
00600      O2=CEXP*H2
00610      O3=-CEXP*H3
00620      O5=-CEXP*H5
00630      SC3O2=SC3*O2
00640      SC4O3=SC4*O3
00650      SC6O5=SC6*O5
00660      PROB=-SC6O5-SC4O3-SC3O2+.5*CX
00670      IF (PROB.LI.0.)STOP
00680      RETURN
00690      END
00700 * THIS PROTOTYPE PROGRAM IS BASED ON MARCOM'S ANALYSIS
00710 * (SUPPLEMENTED BY RCK ANALYSIS) AND INPUTS N INDEPENDANT
00720 * SAMPLES FROM A SQUARE LAW DETECTION OF ADDITIVE NARROWBAND
00730 * GAUSSIAN NOISE AND A CW SIGNAL. ALSO INPUTED IS THE
00740 * SPECIFIED PROBABILITY OF FALSE ALARM PFM. THE PROGRAM
00750 * COMPUTES THE PROBABILITY OF DETECTION FOR VARIOUS
00760 * SIGNAL TO NOISE POWER RATIOS (VARIABLE DB IN PROGRAM). THE RANGE
00770 * OF S/N IS CONTROLLED BY BUILTIN PARAMETERS. DB IS
00780 * RELATED TO DBK USED BY KINCAID AND IS GREATER THAN DB BY
00790 * 10*LOG10(2N).
00800 * THE FUNCTION PROB CONTAINS THE GRAM CHARLIER SERIES
00810 * APPROXIMATION, THE FIRST TERM OF WHICH WOULD BE THE NORMAL
00820 * DISTRIBUTION APPROXIMATION.

```

DISTRIBUTION LIST

Office of Naval Research (2)
Department of the Navy
Arlington, Virginia 22217
Attn: Code 220
Code 222

Director
Naval Research Laboratory
Technical Information Division
Washington, D.C. 20375
Attn: Dr. John Munson

Commander
Naval Undersea Center
San Diego, California 92132
Attn: Mr. G.B. Anderson
Dr. H.A. Schenck

Officer in Charge
Naval Underwater Systems Center
New London Laboratory
New London, Connecticut 06320

Commander
Naval Air Development Center
Warminster, Pennsylvania 18974

Officer in Charge
Naval Ship Research and Development
Center
Carderock Laboratory
Bethesda, Maryland 20034
Attn: Mr. C. Olson

Commanding Officer (2)
Naval Intelligence Support Center
4301 Suttland Road
Washington, D.C. 20390
Attn: STIC 34
Mr. E. Bissett

Officer in Charge
Naval Ship Research and Development
Center
Annapolis Laboratory
Annapolis, Maryland 21402

Commander
Naval Sea Systems Command
Naval Sea Systems Command
Headquarters
Washington, D.C. 20362
Attn: CAPT R. Bruce Gilcrist
(Code 06H2)

Commander
Naval Air Systems Command
Naval Air Systems Command
Headquarters
Washington, D.C. 20361
Attn: Code 533

Commander (3)
Naval Electronic Systems Command
Naval Electronic Systems Command
Headquarters
Washington, D.C. 20360
Attn: CAPT J.C. Bajus, Code 03
CDR H. Miller, Code 320
CAPT D. Jackson (PME 124)

Commander
Oceanographic System, Atlantic
Box 100
Norfolk, Virginia 23511

Commander
Oceanographic System, Pacific
Box 1390
FPO San Francisco 96610

Chief of Naval Operations (2)
Department of the Navy
Washington, D.C. 20350
Attn: OP-951F
CAPT. A.H. Gilmore

Director of Navy Laboratories
Room 1062, Crystal Plaza Bldg. 5
Department of the Navy
Washington, D.C. 20390
Attn: Mr. James Probus

D2

Office of the Assistant Secretary
of the Navy
Department of the Navy
Room 4D745, Pentagon
Washington, D.C. 20350
Attn: Mr. Harry Sonnemann

Office of the Secretary of Defense
DDR&E
Room 3E1044, Pentagon
Washington, D.C. 20350
Attn: Mr. David R. Heebner

Office of the Secretary of Defense (2)
ODDR&E
Room 3D1048, Pentagon
Washington, D.C. 20350
Attn: Mr. Stanley A. Peterson
Mr. Gerald Cann

Mr. A.J. Tachmindji
Advanced Research Project Agency
1400 Wilson Boulevard
Arlington, Virginia 22209
Attn: Doc. Control Rm. 633

Bell Telephone Laboratory (2)
Whippany Road
Whippany, New Jersey 07981
Attn: Dr. Bruce Bogart
Dr. Peter Hirsch

Defense Documentation Center (2)
Cameron Station
Alexandria, Virginia 22314

Institute for Acoustical Research
Miami Division of the Palisades
Geophysical Institute
615 S.W. 2nd Avenue
Miami, Florida 33130
Attn: Mr. M. Kronengold
Dr. J. Clark
Dr. S. Adams
Dr. B. Jobst

General Electric Company
P.O. Box 1088
Schenectady, New York 12301
Attn: Dr. Charles Stutt
Dr. Thomas Kincaid
Dr. Henry Scudder III

General Electric Company
Heavy Military Electronic Systems
Syracuse, New York 13201
Attn: Mr. Don Winfield

Texas Instruments Inc.
13500 North Central Expressway
Dallas, Texas 75231
Attn: Dr. Thomas W. Ellis

Jet Propulsion Laboratory
4800 Oak Grove Drive
Pasadena, California 91103
Attn: Mr. Carl Theile

University of Michigan
Cooley Electronics Laboratory
Ann Arbor, Michigan 48105
Attn: Dr. T.G. Birdsall
Mr. K. Metzgar

Systems Control Inc.
260 Sheridan Avenue
Palo Alto, California 94306
Attn: Dr. L. Seidman